Scintigraphic Imaging of Bacterial and Fungal Infection in Granulocytopenic Rats

Els T.M. Dams, Martin J. Becker, Wim J.G. Oyen, Otto C. Boerman, Gert Storm, Peter Laverman, Siem de Marie, Jos W.M. van der Meer, Irma A.J.M. Bakker-Woudenberg and Frans H.M. Corstens

Departments of Nuclear Medicine and Internal Medicine, University Hospital Nijmegen, Nijmegen; Department of Medical Microbiology and Infectious Diseases, Erasmus Medical Center Rotterdam, Rotterdam; and Department of Pharmaceutics, Utrecht Institute for Pharmaceutical Sciences, Utrecht University, Utrecht, The Netherlands

Scintigraphic imaging in granulocytopenic patients can be very useful to detect and localize infections, which often do not show localizing signs and symptoms. We studied the potential of ^{99m}Tc-labeled polyethylene glycol (PEG)-coated liposomes and ^{99m}Tc-labeled IgG to image bacterial and fungal infection in a granulocytopenic rat model. ^{67}Ga-citrate was used as a reference agent. **Methods:** ^{99m}Tc-PEG-liposomes, ^{99m}Tc-hydrazinonicotinate (HYNIC)-IgG or ^{67}Ga-citrate was administered to granulocytopenic rats with a *Staphylococcus aureus* abscess or with unilateral invasive pulmonary aspergillosis. Imaging and biodistribution studies were performed. **Results:** All agents visualized the *S. aureus* infection from 1 h after injection onward. However, only with ^{99m}Tc-PEG-liposomes and with ^{99m}Tc-HYNIC-IgG did activity in the infectious foci increase with time up to 24 h. ^{99m}Tc-PEG-liposomes and ^{99m}Tc-HYNIC-IgG showed significantly higher accumulation in the infectious focus compared with ^{67}Ga-citrate (1.33 ± 0.31 and 1.40 ± 0.16 percentage injected dose per gram [%ID/g], respectively, versus 0.31 ± 0.04 %ID/g 24 h after injection; $P < 0.05$). At 24 h after injection, abscess-to-muscle ratios were highest for ^{99m}Tc-liposomes (72.1 ± 19.1), followed by ^{99m}Tc-HYNIC-IgG (18.3 ± 3.3) and ^{67}Ga-citrate (4.4 ±0.7). In pulmonary aspergillosis, both ^{99m}Tc-PEG-liposomes and ^{99m}Tc-HYNIC-IgG showed significantly higher uptake in the infected lung than did ^{67}Ga-citrate (3.6 ± 0.4 and 8.3 ± 0.8 %ID/g, respectively, versus 1.3 %ID/g at 24 h after injection; $P < 0.05$). **Conclusion:** ^{99m}Tc-PEG-liposomes and ^{99m}Tc-HYNIC-IgG performed better than did ^{67}Ga-citrate in the localization of peripheral bacterial infection and fungal infection in the lung in granulocytopenic rats. The high focal uptake and high target-to-nontarget ratios of ^{99m}Tc-PEG-liposomes and ^{99m}Tc-HYNIC-IgG indicate that both radiopharmaceuticals may become valuable agents to image infection in granulocytopenic patients.

Key Words: granulocytopenia; infection; imaging; liposomes; immunoglobulin; abscess; aspergillosis

J Nucl Med 1999; 40:2066–2072

Febrile episodes frequently occur in the treatment of cancer patients, particularly during the severe and often protracted neutropenic period induced by aggressive chemotherapeutic regimens. In granulocytopenic patients, >60% of these febrile episodes are of infectious origin, causing substantial morbidity and mortality (*1*). Prompt initiation of empiric broad-spectrum antibiotic therapy has shown improvement in the clinical outcome (*2*). Rapid identification of a possible site of infection helps to tailor the instituted antibiotic regimen and reduces the occurrence of side effects, superinfection and the emergence of resistant microorganisms. However, granulocytopenic patients often lack localizing signs or symptoms, hampering clinical identification of an infectious focus (*3*). Scintigraphic techniques can be useful in the diagnostic process because they provide rapid whole-body evaluation based on functional processes and do not depend on morphologic abnormalities. Imaging with labeled autologous leukocytes is very effective for detection of acute infection (*4,5*) but is obviously not feasible in granulocytopenic patients. Labeled donor leukocytes have been proposed as an alternative method (*6,7*) but are seldom applied because of the high risk associated with human leukocyte antigen immunization, transfusion-associated graft-versus-host disease and transmission of viruses (*8,9*). Therefore, ^{67}Ga-citrate is currently the method of choice for scintigraphic evaluation of the febrile granulocytopenic patient (*10,11*). Opportunistic respiratory infections in particular are adequately visualized with this radiopharmaceutical (*11*). However, imaging with ^{67}Ga-citrate has several disadvantages: The radiopharmaceutical has unfavorable imaging characteristics and causes high radiation exposure; physiologic bowel uptake and accumulation in malignant lymphomas limit its accuracy for the detection of (abdominal) infections; and optimal imaging often requires delayed recordings up to 72 h, whereas a timely diagnosis may have a major clinical impact in these patients.

Several new agents are being developed for imaging of infection. Nonspecific polyclonal human immunoglobulin labeled with ^{111}In has shown high efficacy for visualizing focal infection in both immunocompetent and granulocytopenic patients (*12,13*). A ^{99m}Tc label would be more attractive, providing better image quality and lower radiation exposure. IgG labeled with ^{99m}Tc through the nicotinyl hydrazino derivative hydrazinonicotinate (HYNIC) has shown high accuracy for the detection of clinical infection

Received Sep. 24, 1998; revision accepted Apr. 9, 1999.

For correspondence or reprints contact: Otto C. Boerman, PhD, Department of Nuclear Medicine, University Hospital Nijmegen, P.O. Box 9101, 6500 HB Nijmegen, The Netherlands.

and inflammation (*14*) but, to our knowledge, has not been studied in the granulocytopenic host. Sterically stabilized liposomes, also called polyethylene glycol (PEG)-liposomes, are another newly developed agent in the field of scintigraphic detection of inflammation and infection. The inclusion of PEG into the lipid bilayer of these vesicles results in prolonged blood circulation time compared with conventional liposomes because of reduced uptake by the mononuclear phagocyte system (*15,16*). Experimental studies have shown excellent targeting of inflammatory foci with PEG-liposomes (*17–19*).

In this study, we evaluated the potential of ^{99m}Tc-PEG-liposomes and ^{99m}Tc-HYNIC-IgG to visualize bacterial infection in granulocytopenic rats. In addition, the performance of labeled liposomes and labeled IgG was evaluated in a clinically more relevant model of pulmonary aspergillosis, a frequent and serious fungal infection in immunocompromised patients. For comparison, ^{67}Ga-citrate was included as a reference agent.

MATERIALS AND METHODS

Infection Models

Staphylococcus aureus. A focal *S. aureus* abscess was induced in granulocytopenic rats, as described by Oyen et al. (*13*) with minor modifications. Briefly, male randomly bred Wistar rats, weighing 200–220 g, were injected with one dose of cyclophosphamide (Asta-Medica, Diemen, The Netherlands), 100 mg/kg intraperitoneally, 5 d before bacterial inoculation (day −5), followed by one dose of 75 mg/kg on day −3. The rats had free access to standard rat chow and acidified drinking water. The degree of granulocytopenia was tested in a separate group of five rats. The mean white blood cell count was reduced from 11.3 ± 0.5 × 10^9/L on day −5 to 0.2 ± 0.1 × 10^9/L on day 0 and remained on this level until the end of the experiment. Differential counts showed that <20% of the leukocytes were granulocytes, resulting in a granulocyte count of <0.05 × 10^9/L. Under ether anesthesia, a focal abscess was induced by injecting approximately 1 × 10^6 viable *S. aureus* (ATCC 25923; American Type Culture Collection, Manassas, VA) in 0.1 mL 50%:50% suspension of autologous blood and normal saline in the left calf muscle. Twenty-four hours after the inoculation, when swelling of the muscle was apparent, the respective radiopharmaceuticals were injected through the tail vein.

Pulmonary Aspergillosis. Pulmonary aspergillosis was induced in granulocytopenic rats according to the methods described by Leenders et al. (*20*) with minor modifications. Briefly, female rats (RP strain), 18–25 wk old and weighing 185–225 g, were injected with one dose of cyclophosphamide, 75 mg/kg intraperitoneally, 5 d before fungal inoculation (day −5), followed by one dose of 60 mg/kg on day −1. This protocol resulted in granulocyte counts of <0.1 × 10^9/L on the day of inoculation until the end of the experiment. To prevent bacterial superinfections, animals received ciprofloxacin (660 mg/L) and polymyxin B (100 mg/L) in their drinking water during the entire experiment. Daily intramuscular amoxillin injections (40 mg/kg/d) were added to this regimen starting 1 d before inoculation. Pulmonary infection was established, using a strain of *Aspergillus fumigatus* isolated from an immunocompromised patient with invasive pulmonary aspergillosis. Under general anesthesia, the left main bronchus was intubated. A cannula was passed through the tube, and the left lobe of the lung was inoculated with 2 × 10^4 *A. fumigatus conidia* in a 0.02-mL suspension of phosphate-buffered saline (pH 7.4). This procedure resulted in a left-sided invasive pulmonary infection; signs of mycelial disease were usually seen 16 h after inoculation (*20*). Three rats were inoculated with 0.02 mL normal saline and served as controls.

Radiopharmaceuticals

^{99m}Tc-Polyethylene Glycol-Liposomes. Glutathione-containing PEG-liposomes were prepared as described (*19*). The mean size of the liposome preparations as determined by dynamic light scattering measurements was 100–110 nm with a polydispersity index of <0.1. Preformed glutathione-containing liposomes were labeled with ^{99m}Tc essentially as described (*21*). Briefly, the liposomes (70 μmol phospholipid/mL) were incubated for 15 min at room temperature with freshly prepared ^{99m}Tc-hexamethyl propyleneamine oxime (HMPAO) (6 MBq/μmol phospholipid). Labeling efficiency was between 70% and 80%. Removal of unencapsulated ^{99m}Tc-HMPAO was achieved by gel filtration on a PD-10 column (Pharmacia, Woerden, The Netherlands) with 5% glucose as the eluent. Radiochemical purity as determined on a gel-filtration column (PD-10 column) was >95%.

^{99m}Tc-Hydrazinonicotinamide-IgG. HYNIC was synthesized and conjugated to human polyclonal IgG (Gammagard; Baxter/Hyland, Lessines, Belgium) according to the methods of Abrams et al. (*22*). Approximately one HYNIC group was coupled per IgG molecule, as determined spectrophotometrically. The purified HYNIC-conjugated IgG was diluted to 4 mg/mL in 0.15 mol/L acetate (pH 5.85), sterilized by membrane filtration and stored at −20°C in 0.5-mL aliquots. After thawing 0.5 mL HYNIC-IgG solution, the conjugate was radiolabeled with ^{99m}Tc by adding 0.1 mg *N*-[tris(hydroxymethyl)methyl]glycine (Tricine; Fluka, Buchs, Switzerland), 0.01 mg $SnSO_4$ and ^{99m}Tc-pertechnetate (50 MBq/mg). The mixture was incubated for 15 min at room temperature. The radiochemical purity was determined by instant thin-layer chromatography on silica gel strips (Gelman Science, Inc., Ann Arbor, MI) with 0.15 mol/L acetate (pH 5.85) as the mobile phase. Labeling efficiency was always >95%. High-performance liquid chromatography on a size-exclusion column indicated that the preparation contained <5% aggregates.

^{67}Ga-Citrate. ^{67}Ga-citrate was purchased in kit form (DRN 3103; Mallinckrodt, Inc., Petten, The Netherlands).

Study Design

Staphylococcus aureus Abscess. Twenty-four hours after bacterial inoculation, groups of three rats were injected through the tail vein with 10 MBq ^{99m}Tc-PEG-liposomes, 10 MBq ^{99m}Tc-HYNIC-IgG or 10 MBq ^{67}Ga-citrate. The animals were anesthetized with a mixture of halothane, nitrous oxide and oxygen and were placed prone on a single-head gamma camera equipped with a parallel-hole, low-energy collimator for the ^{99m}Tc studies or a medium-energy collimator for the ^{67}Ga studies. Each group of rats was imaged at 5 min and 1, 2, 4, 10 and 24 h after injection. Images (300,000 counts/image; at 24 h after injection, 100,000 counts/image) were obtained and stored in a 256 × 256 matrix. The scintigraphic results were analyzed by drawing regions of interest over the abscess, the noninfected contralateral calf muscle (used as background region), the heart (representing blood-pool activity) and the whole animal. Abscess-to-background ratios and the percentage of residual activity in the abscess (abscess-to-whole-body ratio) were calculated at various time points. The ex vivo biodistributions of the radiolabels were determined in a separate

experiment. Twenty-four hours after bacterial inoculation, groups of five rats were injected intravenously through the tail vein with 4 MBq ^{99m}Tc-PEG-liposomes, 4 MBq ^{99m}Tc-HYNIC-IgG or 0.4 MBq ^{67}Ga-citrate. Twenty-four hours after injection of the radiopharmaceutical, the rats were killed with 30 mg phenobarbital injected intraperitoneally. Blood was obtained by cardiac puncture. After cervical dislocation, tissue samples (right calf muscle, infected left calf muscle, lung, spleen, kidney and liver) were dissected and weighed, and their activity was measured in a shielded-well scintillation gamma counter (Wizard; Pharmacia-LKB, Uppsala, Sweden). To correct for physical decay and to calculate uptake of the radiopharmaceuticals in each tissue sample as a fraction of the injected dose, aliquots of the injected dose were counted simultaneously. The results were expressed as percentage injected dose per gram (%ID/g). Abscess-to-blood and abscess-to-muscle ratios were calculated.

Pulmonary Aspergillosis. Forty-eight hours after inoculation, groups of six infected rats were injected intravenously through the tail vein with 10 MBq ^{99m}Tc-PEG-liposomes, 10 MBq ^{99m}Tc-HYNIC-IgG or 10 MBq ^{67}Ga-citrate. The noninfected control rats received 10 MBq ^{99m}Tc-PEG-liposomes. Imaging studies were performed as described. The rats were imaged at 2, 8 and 24 h after injection. After obtaining the final image, the rats were killed to determine the ex vivo distributions of the radiolabels. After assessment of macroscopic abnormalities, small samples of the right and left lung were collected for microbiologic examination. The remainders of the right and left lungs were weighed, and their activities were measured in a shielded-well scintillation gamma counter. Tissue samples of other organs were processed as described. Results were expressed as %ID/g. Left-to-right lung, left lung-to-blood and left lung-to-muscle ratios were calculated.

Microbiologic and Histopathologic Studies

Staphylococcus aureus Abscess. S. aureus infection was induced in two granulocytopenic rats and two immunocompetent rats as described. Samples of infected left calf muscle and noninfected right calf muscle were dissected, fixed in formalin and embedded in paraffin. Sections were cut and stained with hematoxylin–eosin for light microscopic examination.

Pulmonary Aspergillosis. Samples of the right and left lungs were aseptically removed. A sample was smeared on Colombia III agar blood plates (Becton Dickinson, Etten-Leur, The Netherlands) that were incubated at 37°C for 48 h to examine possible bacterial coinfection. The remainders of the lung tissues were fixed in buffered formalin. After measurement of radioactivity, the tissues were embedded in paraffin, and histopathologic studies were done on sections that were stained with hematoxylin–eosin or Grocott-Gomori methenamine–silver.

Statistical Analysis

All values are expressed as %ID/g or ratios ± 1 SEM. Statistical analysis of tissue distribution was performed using one-way analysis of variance. Tukey-Kramer multiple-comparison tests were applied. A corrected $P < 0.05$ was considered significant.

RESULTS

Staphylococcus aureus Abscess

Although a relatively small inoculum was used (1×10^6 viable bacteria in granulocytopenic rats versus 1×10^9 viable bacteria in immunocompetent rats), gross swelling of the left calf muscle was apparent in all granulocytopenic rats 24 h after bacterial inoculation. Cross sections of the abscess samples show an encapsulated collection of purulent material. No hemorrhage was observed. Microscopic examination revealed necrosis of muscle tissue but only minimal leukocyte infiltration, in contrast with the massive leukocyte influx seen in immunocompetent rats (Fig. 1). Figure 2 shows the scintigraphic images of the respective radiopharmaceuticals at 1 and 24 h after injection. All agents visualized the abscess as early as 1 h after injection. Furthermore, improved contrast between abscess and background on the subsequent scintigrams was observed with the ^{99m}Tc-labeled agents but not with ^{67}Ga-citrate. Quantitative analysis of the images showed abscess uptake of ^{67}Ga-citrate increased only slightly with time and reached a maximum of 6.8 ± 1.2 %ID at 10 h after injection. The abscess-to-background ratio at 24 h after injection did not exceed 2.0 and was significantly lower than that of the two other agents ($P < 0.01$). In contrast, both ^{99m}Tc-PEG-liposomes and ^{99m}Tc-HYNIC-IgG showed increasing accumulation in the abscess throughout the 24-h period, resulting in significantly higher abscess uptake (16.6 ± 1.9 and 16.3 ± 1.6 %ID, respectively) and abscess-to-background ratios (16.6 ± 1.1

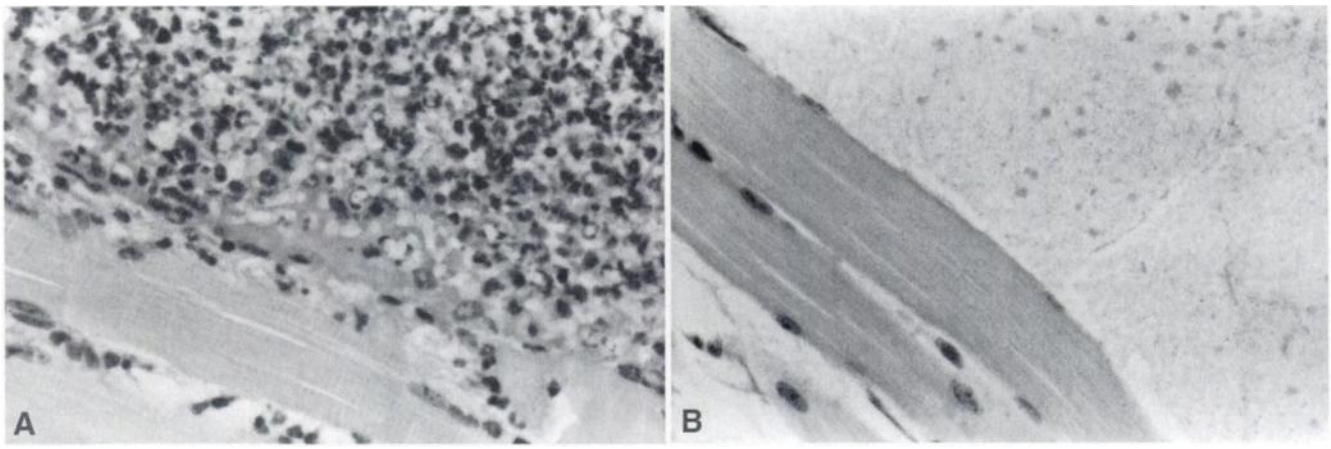

FIGURE 1. Tissue of *S. aureus*-induced abscess in immunocompetent rats (A) and granulocytopenic rats (B). Note massive leukocyte infiltration in A that is not present in B. Hematoxylin–eosin, ×400

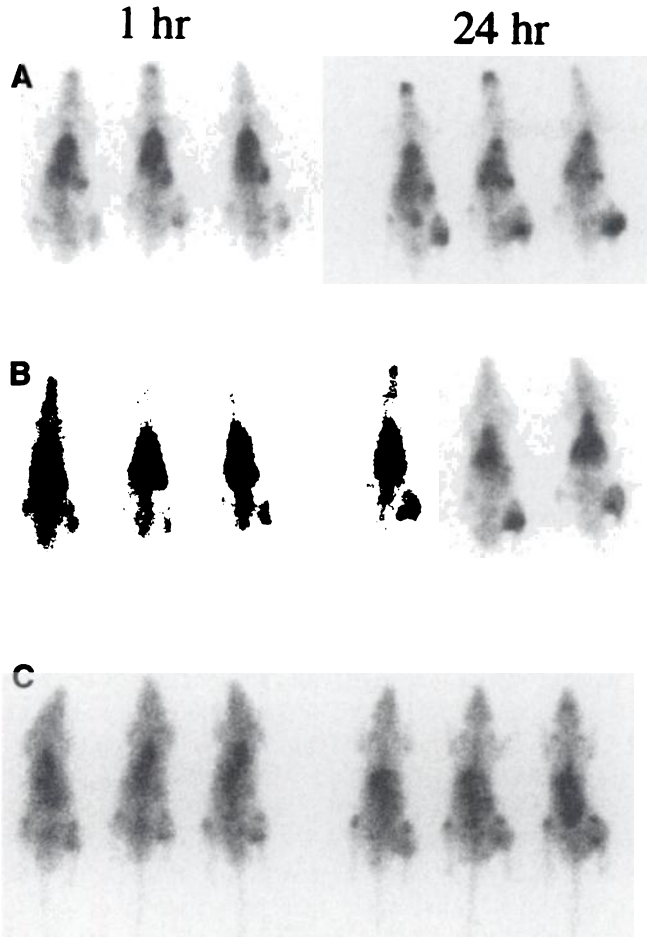

FIGURE 2. Scintigrams of granulocytopenic rats with *S. aureus* infection in left calf muscle imaged at 1 and 24 h after injection of ^{99m}Tc-PEG-liposomes (A), ^{99m}Tc-HYNIC-IgG (B) and ^{67}Ga-citrate (C).

and 12.8 ± 1.4, respectively) compared with ^{67}Ga-citrate ($P < 0.05$). Blood clearance of ^{67}Ga-citrate was significantly faster than that of the ^{99m}Tc-labeled compounds ($P < 0.01$ at 1 h after injection; data not shown): The initial $t_{1/2}$ was approximately 1.5 h compared with approximately 6 and 10 h for the ^{99m}Tc-liposomes and ^{99m}Tc-HYNIC-IgG, respectively.

The biodistribution data of the radiolabels after injection of the three radiopharmaceuticals are given in Table 1. In accordance with the scintigraphic results, ^{99m}Tc-PEG-liposomes and ^{99m}Tc-HYNIC-IgG showed significantly higher uptake in the infectious focus at 24 h after injection than did ^{67}Ga-citrate ($P < 0.05$). The very low uptake of the labeled liposomes in normal muscle resulted in an abscess-to-muscle ratio of 72.1 ± 19.1, 4–16 times higher than the ratios obtained with ^{99m}Tc-HYNIC-IgG ($P < 0.05$) and ^{67}Ga-citrate ($P < 0.01$). Because of the relatively low blood level of ^{67}Ga-citrate, the abscess-to-blood ratio of gallium was higher than for the other two agents ($P < 0.01$). Biodistributions of the three radiopharmaceuticals in the various organs showed relatively high splenic uptake with ^{99m}Tc-PEG-liposomes (5.75 ± 0.74 %ID/g; $P < 0.01$), whereas liver uptake was highest with ^{99m}Tc-HYNIC-IgG (1.06 ± 0.05 %ID/g; $P < 0.001$).

Pulmonary Aspergillosis

Gross hemorrhagic infarctions were macroscopically visible at the base of the infected left lung. In the IgG group, the infarctions appeared to be more extensive than in the other two groups (mean affected lung surface 25% versus 15%), but the difference was not statistically significant. Histologic examination revealed abundant septate branching hyphae invading blood vessels and lung tissue but only minimal leukocyte infiltration (Fig. 3). No mycelial disease was observed in right lung tissue or in lung tissue of the control rats. Negative microbiologic findings excluded bacterial coinfection. The scintigraphic images of the radiopharmaceuticals are shown in Figure 4. At 24 h after injection, increased uptake in the left lung was noted with ^{99m}Tc-liposomes and ^{99m}Tc-HYNIC-IgG. At earlier time points, pathologic uptake in the region of the left lung was not observed unequivocally because adequate delineation of the infection was hampered by the relatively small size of the animals and the vicinity of activity in the cardiac pool. With ^{67}Ga-citrate, minimal uptake was noted in the left lung at all time points. No increased pulmonary uptake was observed in the control rats that had been injected with labeled PEG-liposomes. Quantitative analysis of the images revealed that both ^{99m}Tc-PEG-liposomes and ^{99m}Tc-HYNIC-IgG displayed relatively long half-lives; the absolute values were remarkably higher than those in the *S. aureus* experiment (initial $t_{1/2}$ approximately 20 and 30 h, respectively, versus 6 and 10 h; data not shown).

The biodistribution data of the three radiopharmaceuticals

TABLE 1
Biodistribution of Three Radiopharmaceuticals in Granulocytopenic Rats with *Staphylococcus aureus* Abscess 24 Hours After Injection

Organ	^{99m}Tc-PEG-liposomes	^{99m}Tc-HYNIC-IgG	^{67}Ga-citrate
Blood	0.87 ± 0.06	1.22 ± 0.25	0.07 ± 0.004
Muscle	0.02 ± 0.001	0.08 ± 0.01	0.07 ± 0.01
Abscess	1.33 ± 0.31	1.40 ± 0.16	0.31 ± 0.04
Lung	0.32 ± 0.02	0.72 ± 0.12	0.14 ± 0.01
Spleen	5.75 ± 0.74	2.11 ± 0.16	2.30 ± 0.46
Kidney	2.53 ± 0.20	1.27 ± 0.04	0.44 ± 0.03
Liver	0.58 ± 0.07	1.06 ± 0.05	0.64 ± 0.03
Ratio			
Abscess-to-blood	1.57 ± 0.41	1.29 ± 0.27	4.71 ± 0.66
Abscess-to-muscle	72.1 ± 19.1	18.3 ± 3.3	4.40 ± 0.71
Abscess-to-spleen	0.22 ± 0.03	0.68 ± 0.09	0.16 ± 0.04
Abscess-to-liver	2.28 ± 0.37	1.32 ± 0.10	0.49 ± 0.07

PEG = polyethylene glycol; HYNIC = hydrazinonicotinate.
Values expressed as percentage injected dose per gram ± SEM.

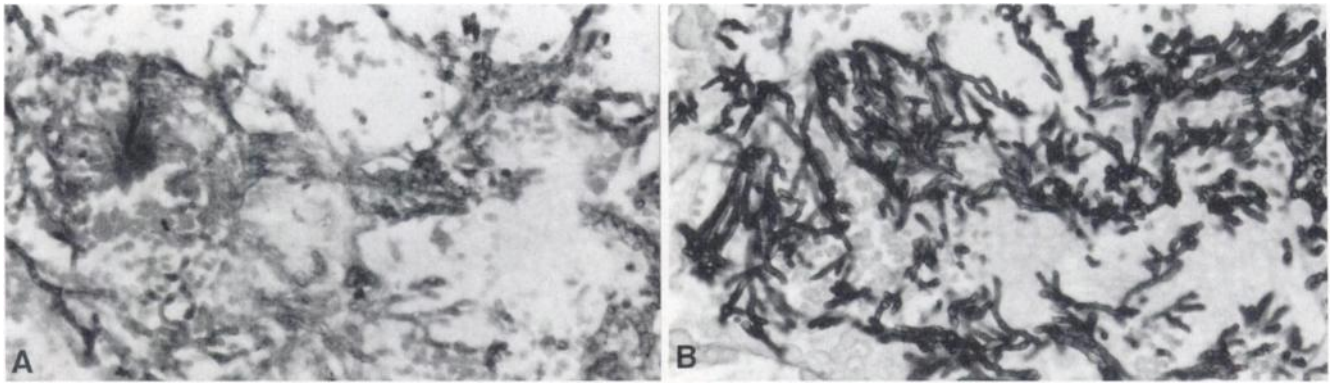

FIGURE 3. Lung tissue of granulocytopenic rats with invasive pulmonary aspergillosis show abundant septate hyphae of *Aspergillus* with only minimal cellular inflammatory infiltration. (A) Hematoxylin–eosin, ×300. (B) Grocott-Gomori methenamine–silver, ×300.

(Table 2) show that uptake in the infected lung was significantly higher with ^{99m}Tc-PEG-liposomes and ^{99m}Tc-HYNIC-IgG than with ^{67}Ga-citrate ($P < 0.05$ and < 0.001, respectively). Because of the relatively high uptake of labeled IgG in normal lung tissue, the liposomes displayed the highest left-to-right lung ratio (3.4 ± 0.4) of the two ^{99m}Tc-labeled agents and also had a higher ratio than did ^{67}Ga-citrate (1.1 ± 0.1). Furthermore, the left lung-to-muscle ratio was significantly higher with the liposomes (96.6 ± 17.1) than with ^{67}Ga-citrate (21.1 ± 5.5; $P <$ 0.001). The left lung-to-blood ratios were similar for the three radiopharmaceuticals. The biodistribution of labeled liposomes in normal lung tissue was similar for rats with or without lung infection. The lung uptake in noninfected tissue was higher than that observed in the *S. aureus* experiment.

DISCUSSION

The paucity of diagnostic clues in the febrile granulocytopenic patient and the limitations of current radiopharmaceuticals stimulate the search for agents capable of rapidly and effectively visualizing infectious foci that are not dependent on the patient's leukocyte count or immune status (or both). This study shows that ^{99m}Tc-PEG-liposomes and ^{99m}Tc-HYNIC-IgG can localize focal bacterial infection in granulocytopenic rats. Compared with ^{67}Ga-citrate, ^{99m}Tc-PEG-liposomes and ^{99m}Tc-HYNIC-IgG had the highest absolute abscess uptake (up to 1.4 %ID/g). A very high abscess-to-muscle ratio (>70) observed with ^{99m}Tc-PEG-liposomes exceeded the values of all other agents. The relatively high uptake of ^{99m}Tc-PEG-liposomes is in line with observations in a previous study (*23*) and most likely is associated with physiologic filtration rather than phagocytosis by spleen macrophages (*24*). In addition to high focal uptake in bacterial infection, labeled PEG-liposomes and labeled IgG also showed preferential accumulation in lung tissue infected with *Aspergillus*. Uptake with these ^{99m}Tc-labeled agents (up to 8.3 %ID/g) was significantly higher than with ^{67}Ga-citrate (1.3 %ID/g). Furthermore, target-to-nontarget ratios exceeded the ratios obtained with ^{111}In-IgG in rats with *Pneumocystis carinii* pneumonia (PCP), another opportunistic respiratory infection (*19*). Because ^{111}In-IgG and ^{67}Ga-citrate have proven their clinical usefulness for detection of these types of infections (*25*), the results of this study hold promise for the clinical application of ^{99m}Tc-labeled liposomes and ^{99m}Tc-HYNIC-IgG for detecting *Aspergillus* infection. The excellent targeting of pulmonary aspergillosis with labeled liposomes is remarkable because this agent failed to localize experimental PCP (*19*). Apparently, the causative microorganism and its histopathologic features affect preferential localization. Invasive pulmonary aspergillosis in granulocytopenic subjects typically shows abundant hyphae and hemorrhagic infarctions with virtual absence of neutrophilic and monocytic lesions (*26,27*), whereas tissue damage is less prominent in PCP and a mononuclear infiltrate prevails (*28*). Perhaps the relatively large size of liposomes in PCP prevents adequate extravasation compared with the smaller IgG molecules.

Currently, a series of radiolabeled peptides (fMetLeuPhe, interleukin-1, interleukin-1 receptor antagonist, interleu-

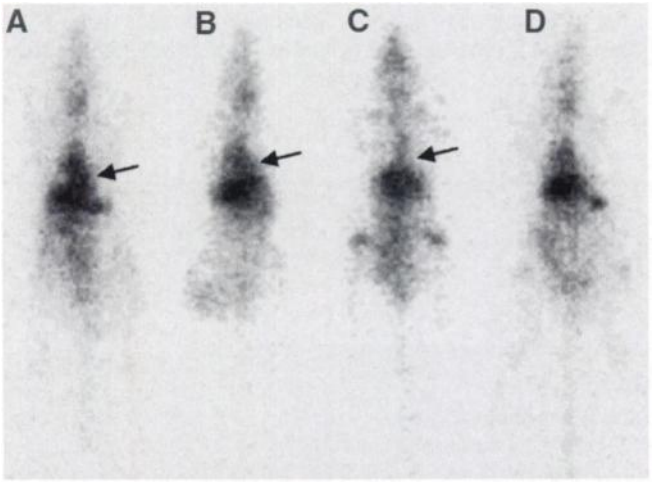

FIGURE 4. Scintigraphic images of granulocytopenic rats with invasive pulmonary aspergillosis 24 h after injection of ^{99m}Tc-PEG-liposomes (A), ^{99m}Tc-HYNIC-IgG (B) and ^{67}Ga-citrate (C). Arrows indicate pathologic uptake in left lung. (D) Noninfected control rat 24 h after injection of ^{99m}Tc-PEG-liposomes.

TABLE 2
Biodistribution of Three Radiopharmaceuticals in Granulocytopenic Rats with Pulmonary Aspergillosis 24 Hours After Injection

Organ	^{99m}Tc-PEG-liposomes (asp)	^{99m}Tc-HYNIC-IgG (asp)	^{67}Ga-citrate (asp)	^{99m}Tc-PEG-liposomes (control)
Blood	2.89 ± 0.25	5.90 ± 0.42	0.65 ± 0.11	2.74 ± 0.97
Muscle	0.04 ± 0.01	0.15 ± 0.01	0.07 ± 0.02	0.13 ± 0.02
Left lung	3.59 ± 0.44	8.31 ± 0.80	1.30 ± 0.36	1.13 ± 0.38
Right lung	1.08 ± 0.10	3.03 ± 0.28	0.55 ± 0.16	1.02 ± 0.38
Spleen	10.60 ± 1.54	7.30 ± 0.73	1.62 ± 0.40	13.28 ± 2.55
Kidney	2.58 ± 0.30	3.21 ± 0.71	2.04 ± 0.34	3.00 ± 0.18
Liver	1.38 ± 0.13	4.18 ± 0.46	1.85 ± 0.35	1.49 ± 0.15
Ratio				
Left-to-right lung	3.4 ± 0.4	2.8 ± 0.3	2.4 ± 0.4	1.1 ± 0.1
Left lung-to-muscle	96.6 ± 17.1	58.2 ± 6.1	21.1 ± 5.5	10.5 ± 5.3
Left lung-to-blood	1.2 ± 0.1	1.4 ± 0.1	2.2 ± 0.7	0.4 ± 0.02

PEG = polyethylene glycol; HYNIC = hydrazinonicotinate; asp = *Aspergillus* infection.
Values expressed as percentage injected dose per gram ± SEM.

kin-2, tuftsin, leukotriene, platelet factor 4, and others) is tested for their ability to image infection and inflammation scintigraphically (*29*). It is anticipated that this approach will eventually lead to a ^{99m}Tc-labeled agent for imaging of infection that will allow rapid and specific localization of infection and inflammation. However, these peptides are directed against receptors expressed on cells that infiltrate in inflammatory foci, and their localization relies on cellular infiltrates. As we have shown in this study, only minimal leukocyte infiltration may occur in neutropenic subjects.

The uptake in the abscess and the abscess-to-muscle ratios of both ^{99m}Tc-PEG-liposomes and ^{99m}Tc-HYNIC-IgG were higher than those reported in previous studies in immunocompetent rats with focal infection (*19,30*). This finding may be related to the stronger inflammatory response seen in neutropenic animals; it has been reported that the proinflammatory cytokine response in neutropenic mice is stronger than in immunocompetent mice (*31*), which may have led to relatively more endothelial damage and vascular leakage. In addition, a stronger outgrowth of bacteria could have occurred in the immunocompromised animals. Still, the results are remarkable because we had to use a relatively low dose of *S. aureus* to avoid overwhelming sepsis and acute mortality (10^6 viable bacteria in granulocytopenic rats versus 10^9 viable bacteria in immunocompetent rats). Obviously, no such comparative data are available for pulmonary aspergillosis. In the *Aspergillus* experiment, the radiopharmaceuticals showed higher uptake in noninfected tissue than in the *S. aureus* experiment, which was probably associated with differences in breed.

The results of this study confirm that localization of labeled IgG and liposomes in infectious foci does not depend on interaction with inflammatory cells because both infection models displayed a conspicuous absence of leukocytes, whereas focal uptake in *S. aureus* abscess was at least as high as in immunocompetent animals. Indeed, several studies have indicated that labeled liposomes and labeled IgG extravasate into inflammatory areas just by virtue of locally enhanced vascular permeability (*32,33*). Thus, the blood level of the radiopharmaceutical is considered to be the driving force for accumulation at the site of infection. Consequently, the improved infection targeting of PEG-liposomes compared with that of conventional liposomes is attributed to their enhanced blood circulation time (*34*).

The moderate performance of ^{67}Ga-citrate in both infection models is remarkable because the usefulness of ^{67}Ga-citrate has been shown for the localization of infectious foci in immunocompromised patients (*11*); however, this study was performed mainly in animals that were not deeply neutropenic. Although the mechanism of ^{67}Ga-citrate concentration in areas of inflammation is subject to debate, lactoferrin present in polymorphonuclear leukocytes has been suggested to bind to ^{67}Ga and thus contribute to focal accumulation (*35*). This concept could possibly explain the performance of ^{67}Ga-citrate in the granulocytopenic rat model.

In view of the histopathologic findings in pulmonary aspergillosis, it is conceivable that, besides increased vascular permeability, focal bleeding may have contributed to focal uptake of labeled liposomes and labeled IgG. This could have biased the results in favor of IgG given the more extensive hemorrhagic infarctions in the IgG group. The contribution of focal bleeding to the uptake of the two agents could be of importance to determine their potential roles in the diagnostic management of *Aspergillus* infection. Although the incidence of infarctions has no relationship to the amount of viable micro-organisms and bleeding can occur early in *Aspergillus* infection (*27*), further studies are needed to evaluate the performance of labeled liposomes and IgG in relation to duration and severity of the disease.

If application under granulocytopenic conditions is feasible, ^{99m}Tc-labeled agents are preferred over ^{67}Ga-citrate—currently the agent of choice for opportunistic infections in immunocompromised patients—because of lower radiation exposure, more favorable imaging characteristics and greater availability. In addition, the higher focal uptake of ^{99m}Tc-PEG-liposomes and ^{99m}Tc-HYNIC-IgG and the higher target-to-nontarget ratios compared with those of ^{67}Ga-citrate suggest improved infection targeting in granulocytopenic patients when these agents are used.

CONCLUSION

In a granulocytopenic rat model, ^{99m}Tc-PEG-liposomes and ^{99m}Tc-HYNIC-IgG provided good visualization of *S. aureus*-induced inflammation early after intravenous injection and showed high focal uptake and target-to-nontarget ratios compared with those of ^{67}Ga-citrate. In granulocytopenic rats with pulmonary aspergillosis, ^{99m}Tc-PEG-liposomes and ^{99m}Tc-HYNIC-IgG showed significantly higher uptake than did ^{67}Ga-citrate. These results indicate that ^{99m}Tc-PEG-liposomes and ^{99m}Tc-HYNIC-IgG might be useful in the evaluation of the febrile granulocytopenic patient and therefore warrant further clinical studies.

ACKNOWLEDGMENTS

The study was supported by grant NGN 55.3665 from the Technology Foundation (Technologiestichting STW), The Netherlands. The authors thank Gerrie Grutters, Bianca Lemmers and Hennie Eikholt for their assistance in the animal experiments; Emile Koenders for his assistance in preparation of the radiopharmaceuticals; and Peter Mast for the hematologic measurements.

REFERENCES

1. Wade JC, Johnson DE, Bustamante CI. Monotherapy for empiric treatment of fever in granulocytopenic cancer patients. *Am J Med.* 1986;80(suppl 5C):85–95.
2. Bodey GP. Infection in cancer patients. *Am J Med.* 1986;81(suppl 1A):11–26.
3. Sickles EA, Greene WH, Wiernik PH. Clinical presentation of infection in granulocytopenic patients. *Arch Intern Med.* 1975;135:715–719.
4. McAfee JG, Thakur ML. Survey of radioactive agents for the in vitro labeling of phagocytic leucocytes. *J Nucl Med.* 1976;17:480–492.
5. Peters AM, Danpure HJ, Osman S, et al. Clinical experience with ^{99m}Tc-hexamethylpropylene-amineoxime for labelling leucocytes and imaging inflammation. *Lancet.* 1986;2:946–949.
6. Dutcher JP, Schiffer CA, Johnston GS. Rapid migration of ^{111}indium-labeled granulocytes to sites of infection. *N Engl J Med.* 1981;304:586–589.
7. Anstall HB, Coleman RE. Donor-leukocyte imaging in granulocytopenic patients with suspected abscesses: concise communication. *J Nucl Med.* 1982;23:319–321.
8. Anderson KC, Weinstein HJ. Transfusion-associated graft-versus-host disease. *N Engl J Med.* 1990;323:315–321.
9. Andreu G, Dewailly J, Leberre C, et al. Prevention of HLA immunization with leukocyte-poor packed red cells and platelet concentrations obtained by filtration. *Blood.* 1988;72:964–969.
10. Tsan M-F. Mechanism of gallium-67 accumulation in inflammatory lesions. *J Nucl Med.* 1985;26:88–92.
11. Palestro CJ. The current role of gallium imaging in infection. *Semin Nucl Med.* 1994;24:128–141.
12. Rubin RH, Fischman AJ, Callahan RJ, et al. In-111-labeled nonspecific immunoglobulin scanning in the detection of focal infection. *N Engl J Med.* 1989;321:935–940.
13. Oyen WJG, Claessens RAMJ, Raemaekers JMM, de Pauw BE, van der Meer JWM, Corstens FHM. Diagnosing infection in febrile granulocytopenic patients with indium-111 labeled human IgG. *J Clin Oncol.* 1992;10:61–68.
14. Dams ETM, Oyen WJG, Boerman OC, et al. Technetium-99m labeled to human immunoglobulin G via the nicotinyl hydrazine derivative: a clinical study. *J Nucl Med.* 1998;39:119–124.
15. Woodle MC, Lasic DD. Sterically stabilized liposomes. *Biochim Biophys Acta.* 1992;1113:171–199.
16. Storm G, Belliot SO, Daemen T, Lasic DD. Surface modification of nanoparticles to oppose uptake by the mononuclear phagocyte system. *Adv Drug Delivery Rev.* 1995;17:31–48.
17. Bakker-Woudenberg IAJM, Lokerse AF, ten Kate MT, et al. Liposomes with prolonged blood circulation and selective localization in *Klebsiella pneumoniae*-infected lung tissue. *J Infect Dis.* 1993;168:164–171.
18. Boerman OC, Storm G, Oyen WJG, et al. Sterically stabilized liposomes labeled with indium-111 for imaging focal infection in rats. *J Nucl Med.* 1995;36:1639–1644.
19. Oyen WJG, Boerman OC, Storm G, et al. Detecting infection and inflammation with technetium-99m-labeled Stealth® liposomes. *J Nucl Med.* 1996;37:1392–1397.
20. Leenders ACAP, de Marie S, ten Kate MT, Bakker-Woudenberg IAJM, Verbrugh HA. Liposomal amphotericin B (AmBisome) reduces dissemination of infection as compared with amphotericin B deoxycholate (Fungizone) in a rat model of pulmonary aspergillosis. *J Antimicrob Chemother.* 1996;38:215–225.
21. Phillips WT, Rudolph AS, Goins B, Timmons JH, Klipper R, Blumhardt R. A simple method for producing a technetium-99m-labeled liposome which is stable in vivo. *Nucl Med Biol.* 1992;19:539–547.
22. Abrams MJ, Juweid M, ten Kate CI, et al. Technetium-99m-human polyclonal IgG radiolabeled via the hydrazino nicotinamide derivative for imaging focal sites of infection in rats. *J Nucl Med.* 1990;31:2022–2028.
23. Boerman OC, Oyen WJG, van Bloois L, et al. Optimization of PEG-liposomes to image focal infection: effects of particle size and circulatory half-life. *J Nucl Med.* 1997;38:489–493.
24. Moghimi SM, Hedeman H, Muir IS, Illum L, Davis SS. An investigation of the filtration capacity and the fate of large filtered sterically stabilized microspheres in rat spleen. *Biochim Biophys Acta.* 1993;1157:233–240.
25. Buscombe JR, Oyen WJG, Grant A, et al. Indium-111-labeled polyclonal human immunoglobulin: identifying focal infection in patients positive for human immunodeficiency virus. *J Nucl Med.* 1993; 34:1621–1625.
26. Berenguer J, Allende MC, Lee JW, et al. Pathogenesis of pulmonary aspergillosis. *Am J Respir Crit Care Med.* 1995;152:1079–1086.
27. Bennett JE. *Aspergillus* species. In: Mandell GL, Bennett JE, Dolin R, eds. *Principles and Practice of Infectious Diseases.* 4th ed. New York, NY: Churchill Livingstone; 1995:2306–2311.
28. Walzer PD. *Pneumocystis carinii.* In: Mandell GL, Bennett JE, Dolin R, eds. *Principles and Practice of Infectious Diseases.* 4th ed. New York, NY: Churchill Livingstone; 1995:2475–2487.
29. van der Laken CJ, Boerman OC, Oyen WJG, van de Ven MTP, van der Meer JWM, Corstens FHM. Scintigraphic detection of infection and inflammation: new developments with special emphasis on receptor interaction. *Eur J Nucl Med.* 1998;25:535–546.
30. Claessens RAMJ, Boerman OC, Koenders EB, Oyen WJG, van der Meer JWM, Corstens FHM. Technetium-99m labelled hydrazinonicotinamido human non-specific polyclonal immunoglobulin G for detection of infectious foci: a comparison with two other technetium-labelled immunoglobulin preparations. *Eur J Nucl Med.* 1996;23:414–421.
31. Netea MG, Kullberg BJ, Blok WL, Netea RT, van der Meer JWM. The role of hyperuricemia in the increased cytokine production after lipopolysaccharide challenge in neutropenic mice. *Blood.* 1997;89:577–582.
32. Morrel EM, Tompkins RG, Fischman AJ, et al. Autoradiographic method for quantification of radiolabeled proteins in tissues using indium-111. *J Nucl Med.* 1989;30:1538–1545.
33. Huang SK, Lee K-D, Hong K, Friend DS, Papahadjopoulos D. Microscopic localization of sterically stabilized liposomes in colon carcinoma-bearing mice. *Cancer Res.* 1992;52:5135–5143.
34. Boerman OC, Oyen WJG, Storm G, et al. Tc-99m labeled liposomes to image experimental arthritis. *Ann Rheum Dis.* 1997;56:369–373.
35. Pauwels EKJ, McCready VR, Stoot JHMB, van Deurzen DFP. The mechanism of accumulation of tumour-localising radiopharmaceuticals. *Eur J Nucl Med.* 1998;25:277–305.